


Article

Improving the Thermal Performance of Indirect Evaporative Cooling by Using a Wet Fabric Device on a Concrete Roof in Hot and Humid Climates

Carlos J. Esparza-López ^{1,*}, Carlos Escobar-del Pozo ², Karam M. Al-Obaidi ^{3,*}
and Marcos Eduardo González-Trevizo ⁴

¹ Faculty of Architecture and Design, University of Colima, Colima 28040, Mexico

² Faculty of Mechanical and Electrical Engineering, University of Colima, Colima 28040, Mexico; cesobar@uclm.mx

³ Department of the Natural and Built Environment, College of Social Sciences and Arts, Sheffield Hallam University, Sheffield S1 1WB, UK

⁴ Faculty of Engineering, Architecture and Design, Autonomous University of Baja California, Mexicali 21100, Mexico; eduardo.gonzalez35@uabc.edu.mx

* Correspondence: cesparza@uclm.mx (C.J.E.-L.); k.al-obaidi@shu.ac.uk (K.M.A.-O.)

Abstract: This study investigated an indirect evaporative cooling system (IECS) to control latent heat loss on roof ponds by increasing the evaporation rates on wet fabric membranes. The cooling potential of the proposed system was experimentally tested in a real environment and it was compared against a roof pond and a floating fiber (gunny bags) to provide an efficient model for buildings in hot and humid climates. Dry bulb temperatures (DBT) are presented for four experimental models. Solar irradiance, ambient and indoor dry bulb temperatures, and relative humidity (RH) were measured for seven days in each of the following climate conditions: hot sub-humid (mean DBT 27.3 °C and mean RH 72%), hot humid (mean DBT 27.1 °C and mean RH 81%), and warm sub-humid (mean DBT 25.2 °C and mean RH 68%). There were no significant variations in thermal performance between the examined devices under hot humid conditions; however, the wet fabric device had superior thermal performance under sub-humid conditions when compared to the other IECSs. In the three climatic scenarios where the proposed system was tested, the wet fabric managed to reduce the indoor air temperature by 6.6 °C, 5.3 °C, and 5.1 °C, respectively, as compared to the outdoor air temperatures.

Keywords: roof pond; passive cooling; wet fabric; experimental testing; indoor thermal performance



Citation: Esparza-López, C.J.; Pozo, C.E.-d.; Al-Obaidi, K.M.; González-Trevizo, M.E. Improving the Thermal Performance of Indirect Evaporative Cooling by Using a Wet Fabric Device on a Concrete Roof in Hot and Humid Climates. *Energies* **2022**, *15*, 2213. <https://doi.org/10.3390/en15062213>

Academic Editors: Athanasios Tzempelikos and Andrea Frazzica

Received: 14 February 2022

Accepted: 14 March 2022

Published: 17 March 2022

Publisher's Note: MDPI stays neutral with regard to jurisdictional claims in published maps and institutional affiliations.



Copyright: © 2022 by the authors. Licensee MDPI, Basel, Switzerland. This article is an open access article distributed under the terms and conditions of the Creative Commons Attribution (CC BY) license (<https://creativecommons.org/licenses/by/4.0/>).

1. Introduction

Evaporative cooling systems are well known and have been widely investigated in the last 20 years. Several studies demonstrated effective passive systems, such as green roofs [1–3], water sprays [4–8], humid porous surfaces [9–11], wet surfaces [12], cool roofs [13,14], or complex hybrid cooling systems [15] are among the variety of passive cooling systems that have shown a cooling potential to achieve comfort conditions over others cooling systems as radiative cooling [16–18] or convective cooling [19–21].

The roof pond system was one of the earliest systems that was studied and developed to avoid solar gains and reduce indoor air temperatures using the indirect evaporative cooling mechanism [22–24]. In recent years, several studies investigated the characteristics of materials, device thickness, and the depth of water to improve the thermal behavior of roof ponds [25,26].

Many variants of roof ponds have been developed to enhance thermal stability by assessing evaporative rate with sprays [14,23] or avoiding solar heat gain by using ventilated self-shaded roof ponds [27,28]. Pearlmuter and Berliner [29] presented a shaded roof pond under hot and dry conditions. Two cells were examined with a flat concrete roof of 0.1 m thickness, with a water layer of 0.02–0.04 m depth, and a lightweight frame

supported by two insulated shade panels at 0.5 m height from the pond. The panels were maintained in a horizontal position through the daytime, but at night, three conditions were tested: (1) closed, (2) partially opened at 45° to improve ventilation, and (3) totally opened and exposed to the night sky. A reduction of 15 °C was achieved; however, the results indicated that the exposure to the night sky is not critical, as their differences were not higher than 1 °C. However, the lowest air temperature was achieved with closed panels during the daytime.

In an effort to improve the thermal efficiency of the pond evaporation rate, solar protection was provided on the surface of the pond to minimize heat gains into the water body and reduce the inner surface temperature compared to the regular pond [22,30]. According to several studies [22,31,32], this variation of roof pond has shown a better performance. Nevertheless, a water layer is still required to maintain the functionality of the system, which presents some complexity in installing the roof that could cause additional structural arrangements to absorb extra loads and neglect the possibility of roof use. The water layer plus the fabric on the surface between the water and the air represents an intermediate step between the roof pond and the proposed system in this research.

Spanaki et al. [25] presented a sensitivity analysis to identify the most relevant parameters that affect the performance of the roof pond with gunny bags. The parameters are relative humidity, water depth, concrete roof slab thickness, gunny bag thickness, emissivity, and absorptivity of the gunny bag. The research established a base case scenario and found that emissivity and the water depth were the most critical parameters affecting the system's efficiency, and the study recommends values of 0.47 for emissivity and 0.2 m for water depth. Nevertheless, the study noted that deep ponds result in extra loads on the concrete slabs, a variable that should be considered in existing buildings or seismic areas.

Aligned with the purpose of increasing the thermal efficiency in roof ponds, 0.08 m of floating insulation was added to the pond in the cool roof system designed by Bourne and Springer [23], reducing 1.1 °C of the indoor air temperature. Nevertheless, the classic roof pond or the variations with sprays, self-shaded or floating fabric as gunny bags presents the best performance in dry climate due to the thermal stability offered by the system according to the thermal requirements of this specific type of climate. Dry climate usually develops extreme air temperatures, as a result, a system that offers thermal stability is necessary to reduce thermal swing between outside and inside conditions.

In contrast, in tropical climates, the evaporative rate from an indirect evaporative cooling system has shown modest benefits [31,33], due to the high levels of humidity in the tropics. The strategies to address this kind of climate should aim to promote real cooling; meanwhile, the heating and heat storage are avoided. Under this premise, a device with thermal stability within the pond is not desirable, however; only controlling the evaporation rate of the water and solar protection of the floating fabric are needed [34].

Esparza et al. [35] demonstrated the cooling potential of a wet fabric system as an evaporative cooling solution using a mathematical model. The study analyzed an indirect evaporative system using a fabric that placed directly on the roof wetted by droppers distributed on the system. The proposed system eliminated the water pond by utilizing the cooling effect of the evaporation, which impacted the roof and removed the thermal stability of the water layer. The simulations showed a maximum reduction in dry bulb temperature of 2 °C in a hot sub-humid condition.

In summary, studies of indirect evaporative cooling on roofs have been investigated primarily in dry climates. The strategy pursued by the system in these climates is mainly about thermal inertia. Consequently, the depth of the water layer has remained between 5 and 30 cm depending on the material of the roof and the climate. In contrast, limited studies have been carried out in humid climates due to the low rate of evaporation and cooling. The strategy in the tropics is contrary to dry climates. Thermal inertia is not desired at all, and the emphasis should be on avoiding heating the system by applying shading devices, surface properties, or floating elements on the surface of the water; and improving the cooling rate by increasing evaporation. Consequently, reducing the depth of

the water layer to a minimum while maintaining its evaporation capacity appears to be a promising solution.

Therefore, this study aims to experimentally assess the thermal performance of a wet fabric device by reducing the water level to a minimum and comparing it against roof pond and floating fiber to provide an efficient cooling model for buildings in hot and humid climates. Indoor dry bulb temperature was measured for the three cooling solutions. Outdoor dry bulb temperature, relative humidity, and solar irradiance were recorded for three different climates in Colima, México: hot humid, hot, and warm sub-humid conditions. The cooling performance of the wet fabric device was determined in comparison with a reference test cell; furthermore, experimental results were used to quantify the thermal performance of each device.

2. Materials and Methods

This research assesses the thermal performance of three evaporative cooling devices on a concrete roof: roof pond, roof pond with a floating fabric also known as gunny bags, and a wet fabric. The roof pond or water pond consists of a water layer on the roof. The floating fabrics or gunny bags incorporate a layer of fabric or textile on the surface of the water. The wet fabric reduces the water layer on the roof to the minimum but still incorporates the fabric to retain the water. The three devices were installed on test cells, which are described below. The thermal behavior of the cooling devices was compared to a reference cell.

In Figure 1, a method scheme of the research is presented. It indicates the experimental cells used in the three climatic conditions. It also summarizes the calibration campaign in two different steps: to calibrate the equipment using the micro-station as a reference then validate the experimental cells using one of the calibrated data loggers. The climatic conditions are defined in Section 2.1. The characteristics of the cells are presented in Sections 2.2 and 2.3. The characteristics of the equipment are presented in Section 2.4.

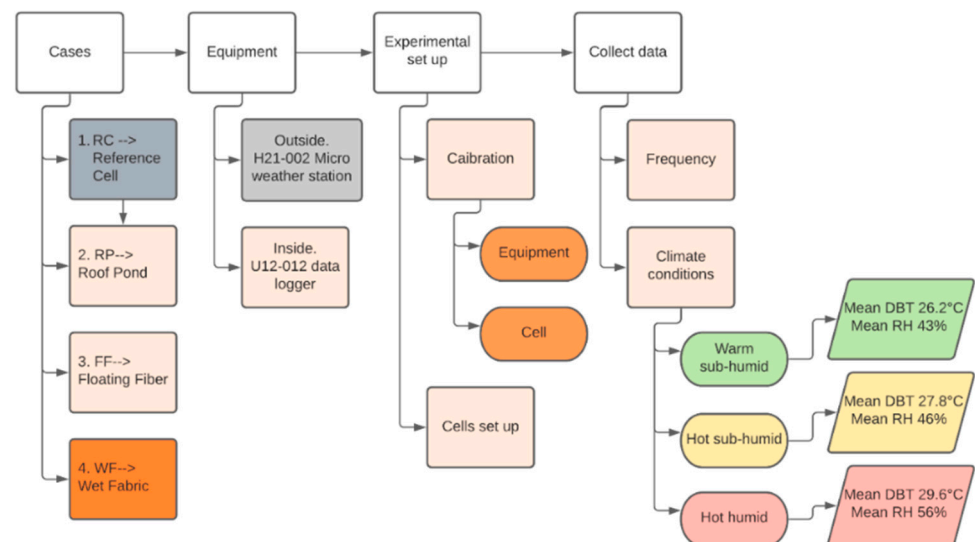


Figure 1. Research process demonstrated by selected variables and methods.

2.1. Location

The research was conducted in Coquimatlan, Colima, Mexico. The geo-positioning coordinates are 19°12'41" north latitude, 103°48'23" west longitude, and over 354 masl. The region is classified as Aw tropical wet or savanna according to Köppens climate classification [36]. Figure 2 summarizes the monthly maximum, mean, and minimum dry bulb temperature (DBT) and the monthly maximum, mean, and minimum relative humidity (RH) for the city of Coquimatlan.

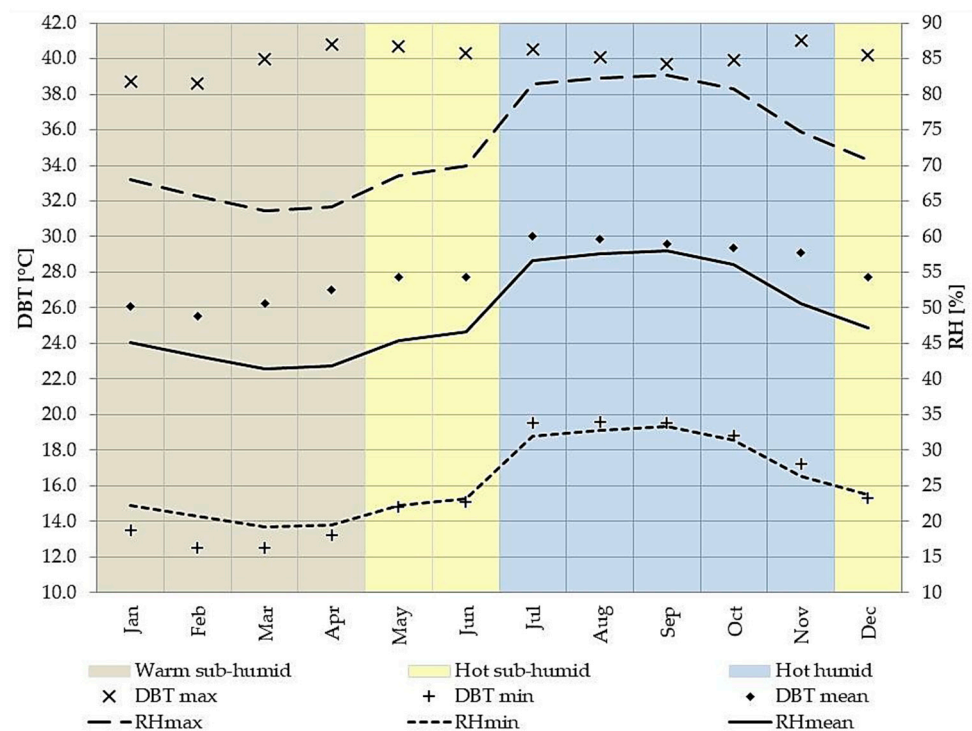


Figure 2. Monthly dry bulb temperature and relative humidity for Coquimatlan, Mexico.

The climatic conditions were grouped under three different environments according to their similarity in terms of temperature and RH: (1) warm sub-humid (light brown) from January to April with a mean DBT of 26.2 °C and a mean RH of 43%; (2) hot sub-humid (yellow) in the months of May, June, and December with a mean DBT of 27.8 °C and mean RH of 46%; and (3) hot humid (light blue) from July to November with a mean DBT of 29.6 °C and mean RH of 56%. The experiment was carried out during one week of each climate condition. The targeted months for the trials were February, May, and October.

2.2. Experimental Cells

Four identical cells were used simultaneously to test the three devices and the reference cell. The distribution of the cells was arranged as shown in Figure 3. The reference cell (RC) was located at the northeast corner of the experimental area, floating fabric (FF) was placed over the northwest cell, the wet fabric (WF) over the southeast cell, and the roof pond (RP) over the southwest cell. The constructive characteristics of the cells are listed in Table 1.

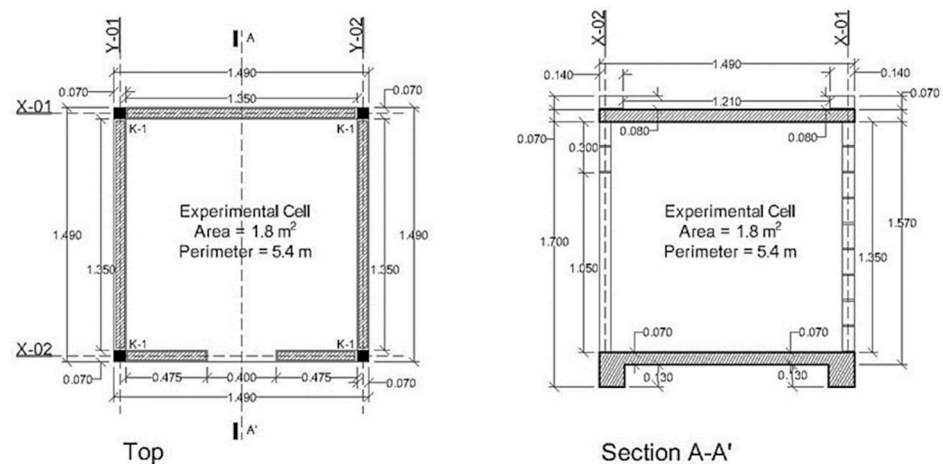


Figure 3. Left: distribution of the four experimental cells. Right: photo of the experimental area.

Table 1. Constructive specifications of the experimental cells.

Elements	Description	U Value
Floor	0.07 m of reinforced concrete slab directly placed over the compacted ground.	$3.19 \text{ Wm}^{-2}\text{K}^{-1}$
Walls	0.07 m of clay bricks. Outside faces were plastered with 0.015 of mortar and 0.04 m of polystyrene plates. Inside faces were left with an apparent clay brick finish.	$0.76 \text{ Wm}^{-2}\text{K}^{-1}$
Roof	0.08 m of a reinforced concrete slab.	$2.95 \text{ Wm}^{-2}\text{K}^{-1}$

Internal dimensions of the cells are $1.35 \text{ m} \times 1.35 \text{ m} \times 1.35 \text{ m}$ (Figure 4). These dimensions are according to a scale of 1:2 of the minimum dimensions allowed from the current local construction normative. All cells have an opening in the north façade of $0.40 \text{ m} \times 1.05 \text{ m}$ at ground level as an entrance. Over the roofs, a parapet made of clay bricks of 0.14 m thick and 0.08 m high was constructed all over the perimeter. The roofs have a 1% slope to drain rainfall in the south façade by a spout.

**Figure 4.** Top and section drawings of the test cell.

To minimize the heat transfer between the exterior and the interior through the walls, 0.04 m of polystyrene plates (U value of the walls $0.76 \text{ Wm}^{-2}\text{K}^{-1}$) were positioned in the four walls as insulation (Figure 5). The door of each cell was made of two sheets of polystyrene of 0.05 m. The fitting of the polystyrene sheets and sailed door was made according to the standard ASTM C-1046 [37]. All the roofs were protected with a white acrylic waterproof application.

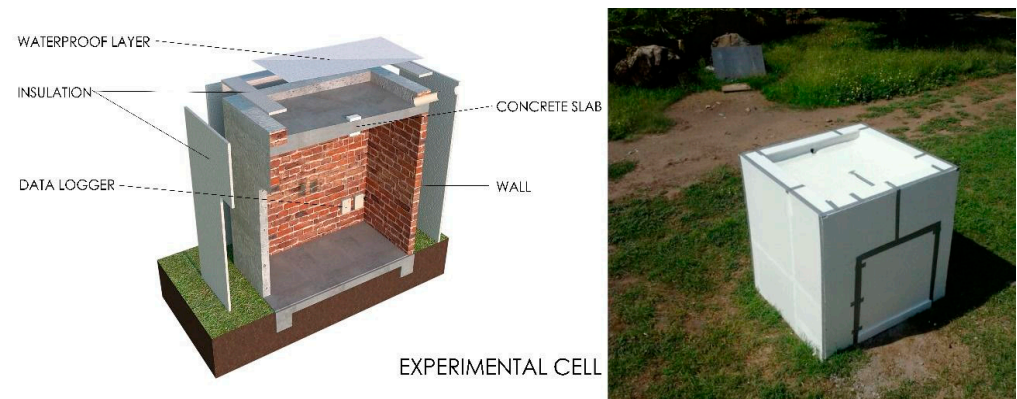


Figure 5. Cross section diagram of the experimental cell with its elements.

2.3. Scenarios

2.3.1. Roof Pond

For this experiment, a mean water depth layer of 0.05 m was used over the roof (Figure 6). Several authors [23,30,38,39] agree that the water depth to achieve the best performance for concrete roofs with roof ponds and floating fabric is approximately 0.05 m. Therefore, to keep the scenarios as similar as possible to previous studies, the roof pond and floating fabric water depth used was 0.05 m. The total volume of water placed over the roof was 0.09 m³.

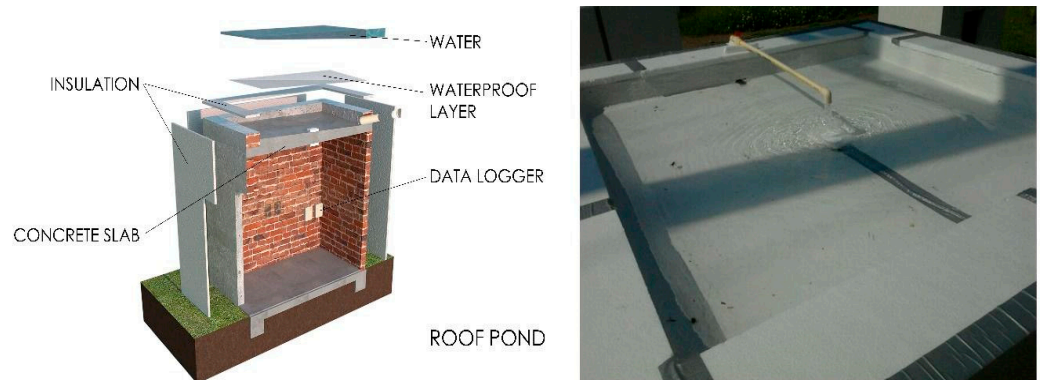


Figure 6. Cross section diagram of the roof pond cell with its elements.

2.3.2. Floating Fabric

The second case was the floating fiber or gunny bags. The cell characteristics remained identical to the roof pond except for the floating device. The floating device was made of a perforated polystyrene sheet of 0.025 m as shown in Figure 7. Over the floating device, a white woven membrane of 0.003 m made of wool fabrics and polyester was laid down.

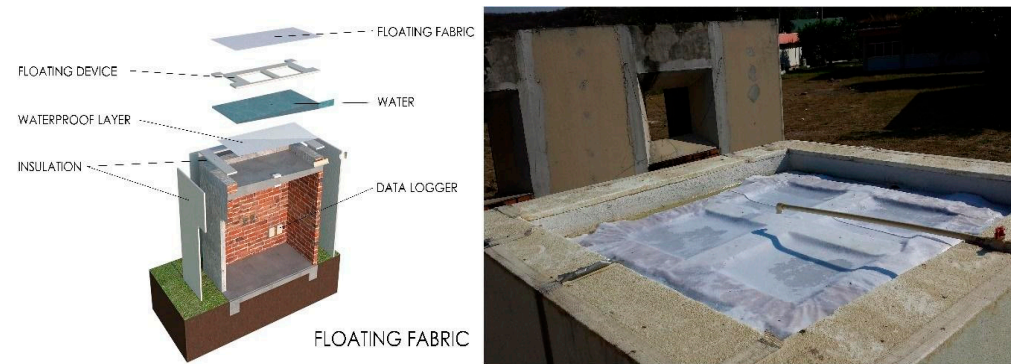


Figure 7. Cross section diagram of the floating fiber or gunny bag cell with its elements.

2.3.3. Wet Fabric

The proposed innovation in this study is the reduction of the water layer to keep the cooling process of the evaporation right above the roof. The setting of the membrane placed directly over the roof allowed it to retain a thin film of water until it evaporated totally. Besides helping to keep the water film, the membrane reduces the heat flux incoming to the roof and improves the evaporation ratio due to the increase of the contact area between the air and the water [40].

To keep wetting the membrane all the time, droppers were installed over the roof, as shown in Figure 8. Four droppers were distributed equidistantly over the surface, i.e., 0.68 m between each droplet and 0.34 m from the edge, and connected to a water supply made of a CPVC pipe of 19.05 mm diameter. The pipeline was insulated with 0.05 m of foam insulator to avoid heating from solar irradiance. The droppers supplied 2 L/h each and the excessive amount of water was drained out by the slope through the spout.

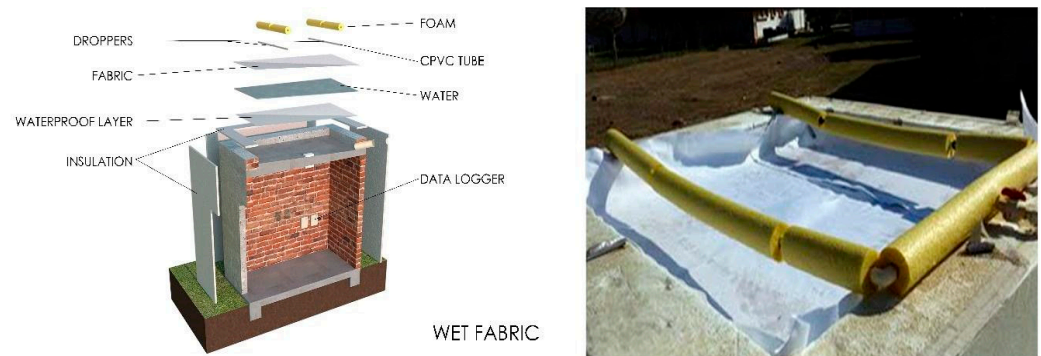


Figure 8. Cross section diagram of the wet fabric cell with its constructive characteristics.

2.4. Equipment

The outdoor variables were the dry bulb temperature (DBT), relative humidity (RH), and solar radiation. The equipment used to collect the data from the outdoor was a data logger micro-station H21-002 Onset comp. An additional plug-and-play S-THB-M002 Temperature/Relative Humidity smart sensor was connected to the micro-station. The specifications of the sensor are measurement range from $-40\text{ }^{\circ}\text{C}$ to $75\text{ }^{\circ}\text{C}$ with $\pm 0.21\text{ }^{\circ}\text{C}$ accuracy and resolution of $0.02\text{ }^{\circ}\text{C}$ for temperature and 0% to 100% with $\pm 2.5\%$ accuracy and resolution of 0.1% for RH. In addition, a silicon pyranometer sensor was plugged into the micro-station. The specifications are measurement range from 0 to 1280 Wm^{-2} , operating temperature range from $-40\text{ }^{\circ}\text{C}$ to $75\text{ }^{\circ}\text{C}$, an accuracy of $\pm 10\text{ Wm}^{-2}$, resolution of 1.25 Wm^{-2} , and spectral range from 300 to 1100 nm. The location of the outside sensor was in the middle of the four experimental cells in the xy-axes and at 3.5 m high in the z-axis.

The variable logged inside the experimental cells was the DBT. The equipment used was a data logger U12-012 Onset Comp. Its specifications are measurement range from $-20\text{ }^{\circ}\text{C}$ to $70\text{ }^{\circ}\text{C}$, an accuracy of $\pm 0.35\text{ }^{\circ}\text{C}$, and resolution of $0.03\text{ }^{\circ}\text{C}$. The location of the data logger was at the center of the cells, as can be seen in Figures 5–8, according to the ASTM standards [37,41–43], i.e., 0.675 m distanced of each inner surface. The frequency of the data collection was every hour for seven days for each climatic condition.

3. Results

3.1. Warm Sub-Humid Climatic Condition

The results of the warm sub-humid season are presented in this section. Figure 9 presents the measurements of indoor DBT for each cell, as well as the outdoor conditions: DBT (black) and solar irradiance (red) during seven days. The RH levels for this season swung between 43% and 94%. The three devices (green, purple, and light blue) were tested to perform similarly day and night. Through the week, the three devices presented lower maximum, mean, and minimum DBT than the reference case (gray) without any device.

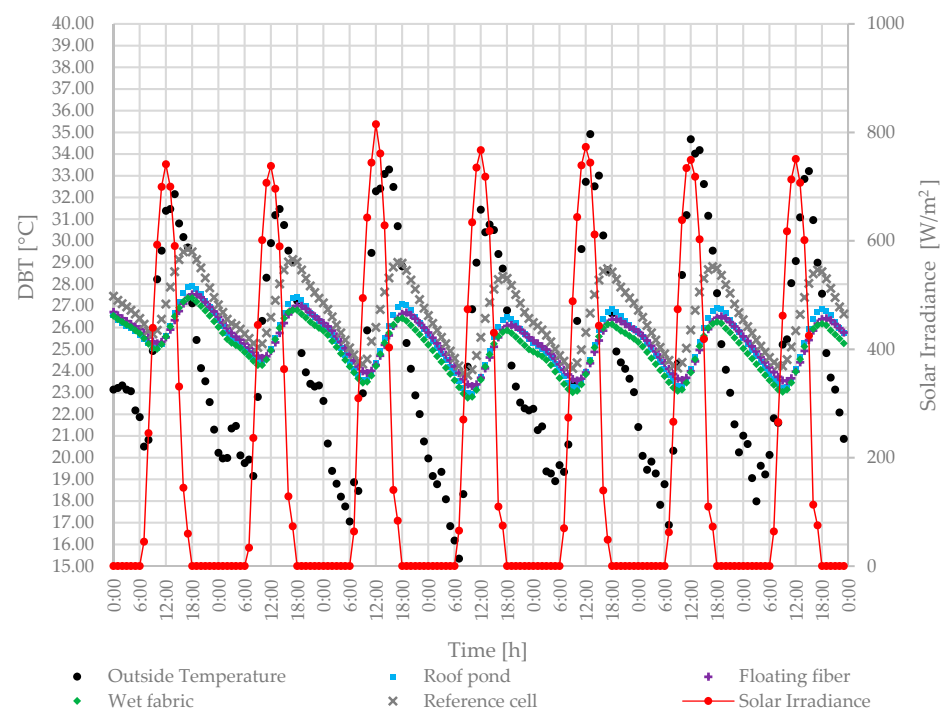


Figure 9. Comparison of the indoor air temperatures in the warm sub-humid season.

Figure 10 shows the average, maximum, and minimum indoor DBT for all the tested cells as well as the outdoor DBT. It also shows the daily maximum average (upper circle in the box) and the daily minimum average (bottom circle in the box). Finally, the boxes represent the first and third quartiles of the measured data. As can be seen in Figure 10, the devices achieved a notable reduction of maximum DBT in comparison to the reference cell. In addition, the three devices damped the thermal swing, although the average for outdoor was lower than for the indoor DBT for all cases.

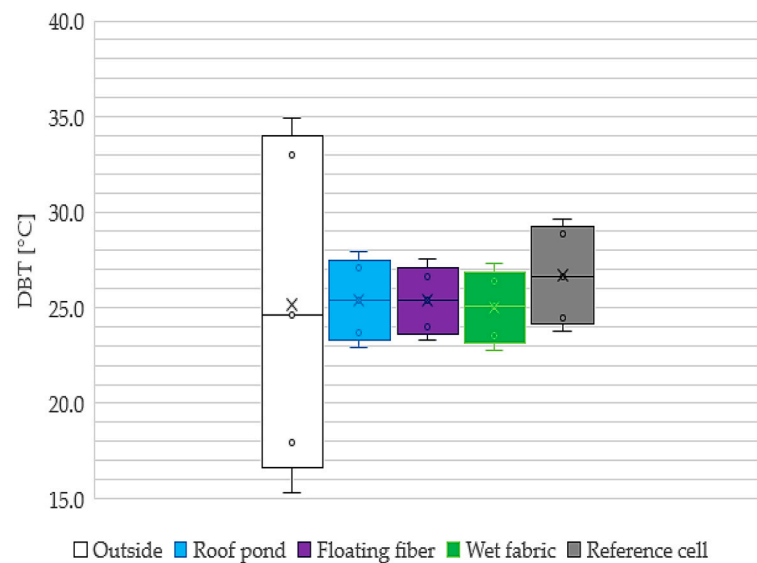


Figure 10. Box plot of the indoor air temperatures in the warm sub-humid season.

The maximum DBT of the three devices is maintained under the maximum DBT of the reference cell by approximately 2 °C. The minimum average DBT for the three devices is similar for the measured period. The mean temperatures of the RP (blue box), FF (purple box), and WF (green box) were 1.2 °C, 1.3 °C, and 1.6 °C below the RC (gray box) mean DBT, respectively. It is important to notice that the maximum temperatures of the three devices were quite close to the mean DBT of the reference cell. Concerning the maximum reduction, the RP, FF, and WF performed 1.8 °C, 2.2 °C, and 2.5 °C below the RC maximum and 6.0 °C, 6.4 °C, and 6.6 °C below the outdoor maximum.

3.2. Hot Sub-Humid Climatic Condition

The outdoor RH was between 44% and 90%. The outdoor DBT swing was between 20.5 °C and 34 °C, as can be seen in Figure 11. A typical day for this season was presented at the midweek. Solar irradiance reduction confirmed a cloudy day with rain causing the decrement of all the temperatures.

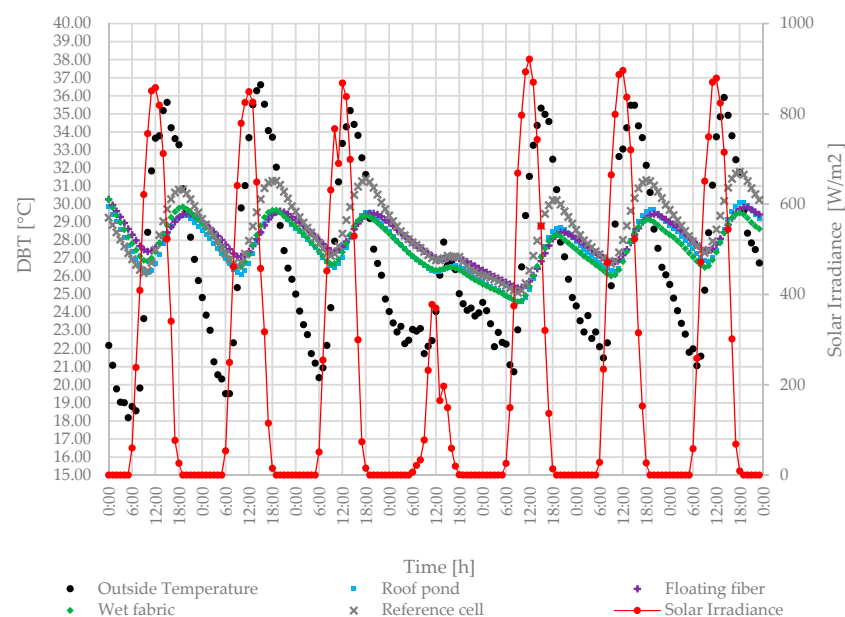


Figure 11. Comparison of the indoor air temperatures in the hot sub-humid season.

In this season, the thermal performance of the three devices was similar to the last season. Additionally, the maximum DBT of the reference cell presented a higher record than the device's maximum DBT. The mean values of DBT devices presented a reduction of 0.9 °C, 0.5 °C, and 0.9 °C for RP, FF, and WF, respectively, against the mean record of the reference cell.

The maximum DBT values, RP, FF, and WF presented a decrement of 1.5 °C, 1.4 °C, and 1.7 °C in comparison with the RC, respectively, and 5.2 °C, 5.1 °C, and 5.3 °C, respectively, taking the outside DBT as a reference. The general performance of the devices is consistent with the performance of the previous climate season. It can be observed that the differences between the devices are marginal but slightly better than the RP and WF over the FF (Figure 12).

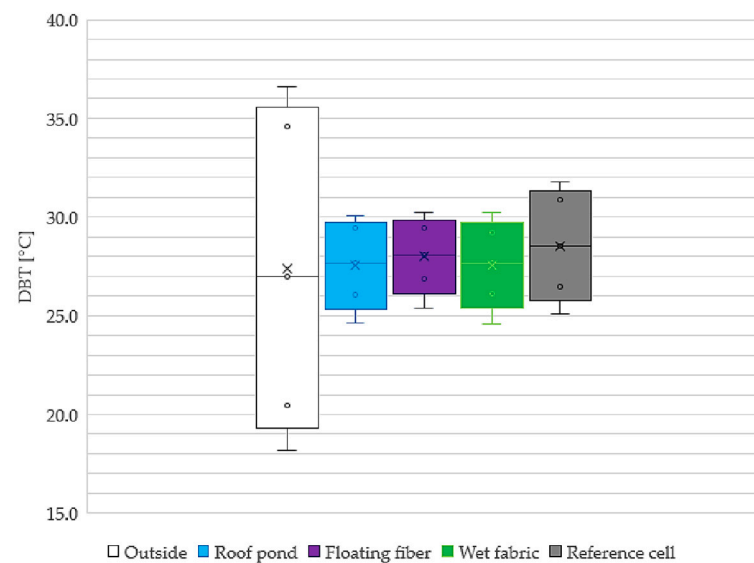


Figure 12. Box plot of the indoor air temperatures in the hot sub-humid season.

3.3. Hot Humid Climatic Condition

For the hot humid season, the RH swing was between 66% and 96%, considerably higher than the previous two climate types. During the experimental stage, there was a gap of six hours where all the equipment did not work during the first day. In addition, the pyranometer suffered a failure that resulted in missing the solar irradiation data for the first three days. However, the last four days of the experimental period are fully presented in Figure 13. On the sixth day of the experiment, it was cloudy near noon, making the solar irradiance drop down to 240 Wm^{-2} .

The thermal performance of the three devices was quite similar throughout this season. The average differences between the maximum values were 0.1 °C, 0.4 °C, and 0.4 °C for the RP, FF, and WT, respectively, regarding the reference cell. In contrast, taking outside DBT as a reference, the differences were 4.8 °C, 5.1 °C, 5.1 °C, and 4.6 °C for the RP, FF, WT, and RC, respectively.

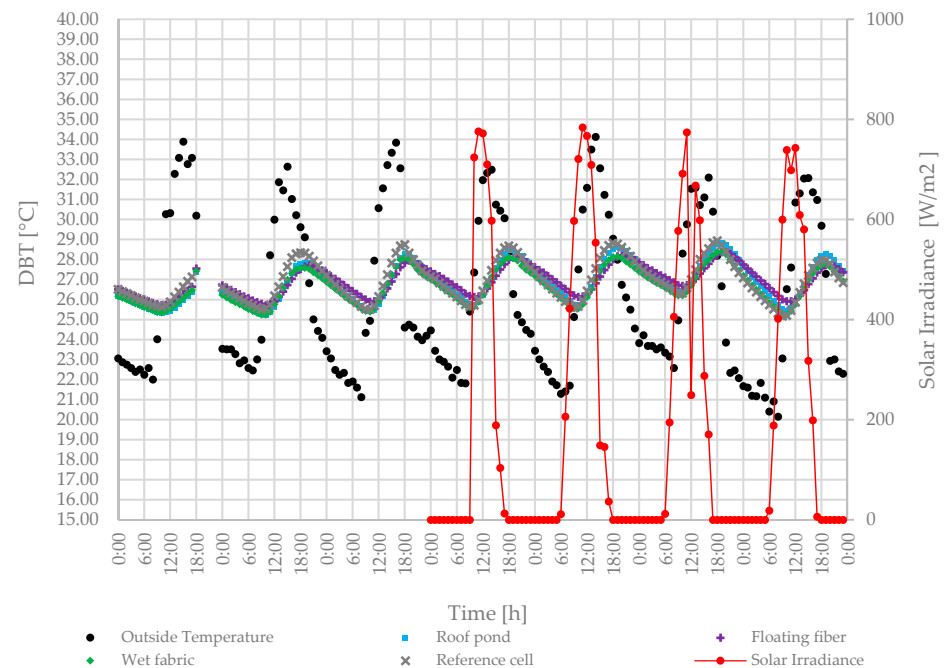


Figure 13. Comparison of the indoor air temperatures in the hot humid season.

Figure 14 shows the average performance of the experimental cells and the outdoor DBT. The differences of the mean values were 0.7 °C, 0.8 °C, 0.5 °C, and 0.8 °C for the RP, FF, WF, and RC, respectively. The WF was the device with better performance over the other devices, with a marginal difference of 0.2 °C or 0.3 °C.

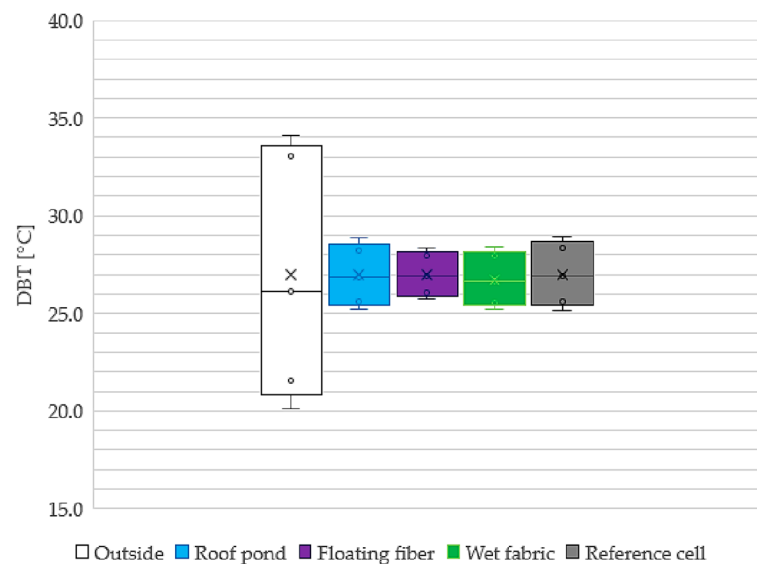


Figure 14. Box plot of the indoor air temperatures in the hot humid season.

3.4. Comparison of Different Climatic Conditions

To compare the results of the three climate types, the thermal swing performance is presented in Figure 15. The roof pond, floating fiber, and wet fabric reduce the thermal swing by 22.7%, 38.6–40.9%, and 34.1–29.5%, respectively, for the warm sub-humid and hot sub-humid seasons in comparison with the thermal swing of the reference cell. For the hot humid season, the floating fiber showed a greater reduction of the thermal swing of 32.1%; the wet fabric and the roof pond reduced it by 14.3% and 7.1%, respectively. It is well

known that a water pond reduces thermal oscillations; however, the results revealed that the combination of the fiber shading plus the water pond has a strong influence controlling the thermal swing.

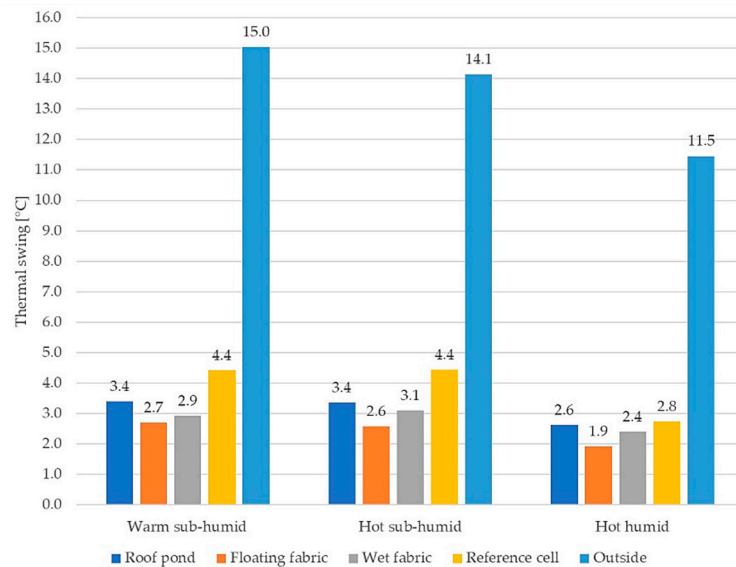


Figure 15. Thermal swing of all cases in the three climatic conditions.

Figure 16 presents the mean DBT including outdoor values. The WF cell showed the lowest mean DBT of all the devices in the three climatic conditions. The reduction of the mean values was 1.5 °C, 0.9 °C, and 0.3 °C for the warm sub-humid, hot sub-humid, and hot humid, respectively, compared to the reference cell.

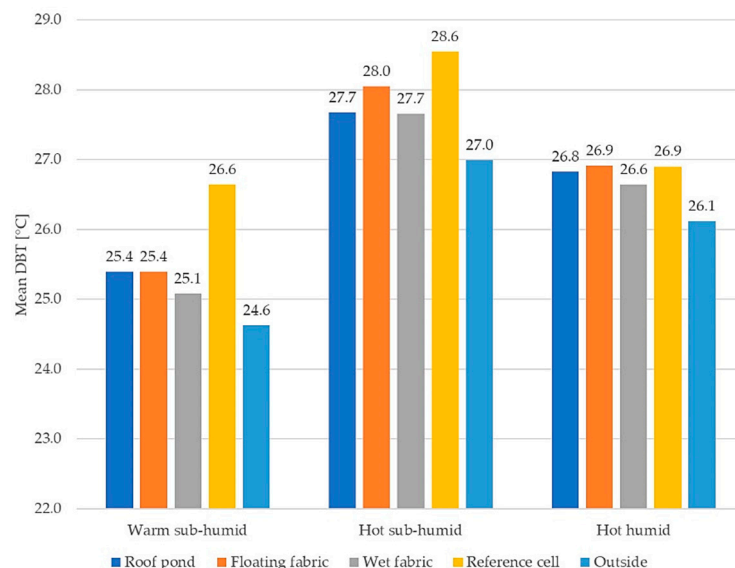


Figure 16. Mean DBT of all cases in the three climatic conditions.

To compare the results regardless of whether they were from different measurements trials, the temperature difference ratio (TDR) was utilized. It was first proposed by Givoni and then used by several authors [2,3,44] to compare the same system or device in different

periods. The TDR indicates the fraction of reduction of the maximum temperature in function of the outside thermal swing. The equation to calculate this value is presented below:

$$\text{TDR} = \frac{(\text{DBT}_{\text{maxout}} - \text{DBT}_{\text{maxin}})}{(\text{DBT}_{\text{maxout}} - \text{DBT}_{\text{minout}})} \quad (1)$$

where

$\text{DBT}_{\text{maxout}}$: DBT outside maximum

$\text{DBT}_{\text{maxin}}$: DBT inside maximum

$\text{DBT}_{\text{minout}}$: DBT outside minimum.

A higher value of TDR indicates a better performance indoor compared to the outdoor thermal swing. If the value overpasses 50%, it indicates a real cooling or sensible cooling inside the experimental cell compared with DBT outdoor conditions.

Figure 17 shows the TDR for all experimental cells in the three climatic conditions. The values show again that the device with the best performance is the WF. In the three seasons, the TDR remained over 40%. The main differences can be observed in the warm sub-humid season where the WF achieved a 43.5% reduction compared to the 42% of the FF, 39% of the RP, and the 27% of the RC.

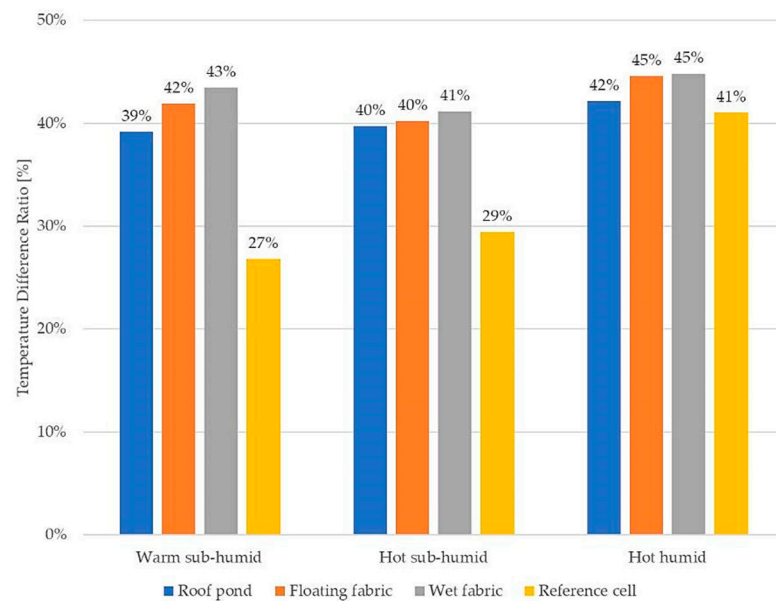


Figure 17. Temperature differences ratio of devices in the three climatic conditions.

In general, the FF and the WF performed quite similarly in the three periods of the experimental process and there is a marginal difference, which indicates the best performance of the WF. These results highlight the importance of the membrane to reduce the effect of solar irradiance heat flux inside the building.

The results showed a reduction of maximum temperatures in the sub-humid conditions compared to the reference cell. The reduction of the maximum values in the humid season was marginal due to the RH in the ambient that reduces the ability of the devices to evaporate and cool down the indoors.

Finally, the representative day (RD) [45] of each climatic condition is presented for the wet fabric to show the evolution of the system through 24 h. The RD is calculated as the next equation indicates:

$$|T_{\text{mdaily}} - T_{\text{mseason}}| + |S_{\text{mdaily}} - S_{\text{mseason}}| \cong 0 \quad (2)$$

where T_{mdaily} is the mean DBT of each day recorded, $T_{mseason}$ is the mean DBT of the climatic condition or season, S_{mdaily} is the thermal swing of each day recorded, and $S_{mseason}$ is the thermal swing of the climatic condition or season. The process to identify the RD is to analyze each recorded day with the data of its climatic condition to obtain the summary of DBT and thermal swing. The representative day of each climatic situation was the one with the closest value of each analysis to zero as it presents the lowest differences of DBT and thermal swing and represents its performance more like the performance of that period.

Figure 18 presents the RD of the wet fabric through 24 h performance over the three climatic conditions. In this figure, the maximum, minimum, and thermal swing of outdoor and wet fabric DBT are presented. The sub-humid conditions (blue and green) present the outdoor DBT highest thermal swing with 17 °C and 17.5 °C for hot and warm, respectively. With the highest RH in the environment, the thermal swing used to drop down, as can be seen in the humid condition (yellow) with 13 °C. The performance inside the experimental cell was similar in the three climatic conditions in terms of thermal swing. They presented a thermal swing of approximately 3.5 °C.

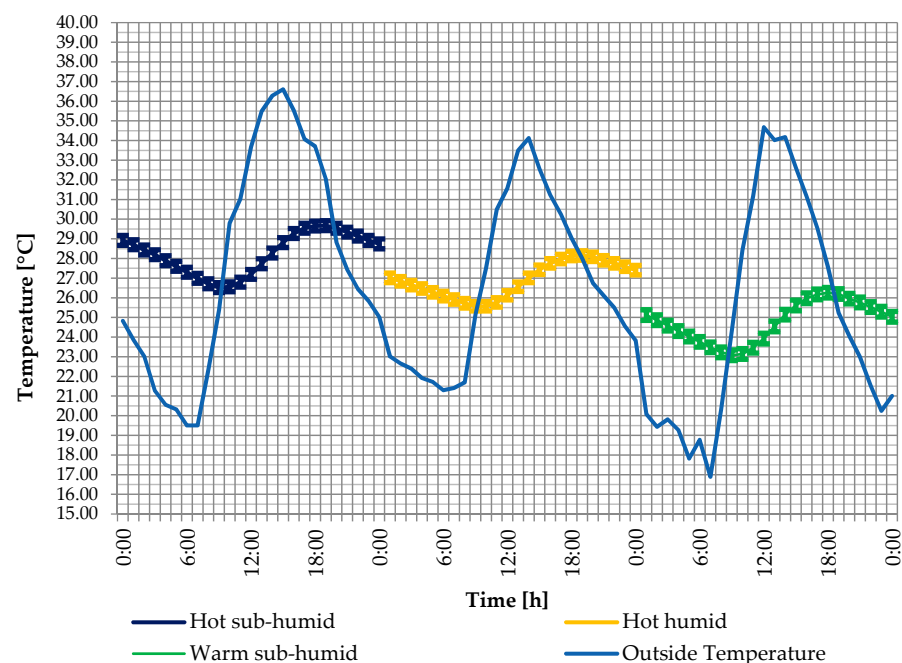


Figure 18. Representative day of the wet fabric performance in the three climatic conditions.

The main differences are in minimum and maximum values. For hot conditions, minimum values were approximately 25.5 °C for hot humid and 26.5 °C for hot sub-humid, and maximum values of 28.3 °C and 29.6 °C, respectively. In warm conditions, these values were lower than in hot conditions, with a minimum of 23 °C and maximum of 26.3 °C.

4. Discussion

As several studies indicated, water depth is a critical parameter at the moment to design roof ponds. There is a wide range of water depth recommendations in the literature depending on the characteristics of the roof and climatic conditions. For roofs with high inertia materials, great depth is not as necessary as would be for high conductivity materials [14,23,28]. Additionally, outdoor climatic conditions and strategies to achieve indoor climatic requirements determine water depth. For dry climates, extreme temperatures are presented through nighttime and daytime, so a strategy is to drop down thermal swing with high inertia provided by a large amount of water. In wet climates, high temperatures are presented all day long and thermal swing is lower. Therefore, the strategy to apply

is cooling instead of reducing thermal swing, so water depth should be lower to avoid storing heat.

Spanaki et al. [22] recommended 0.30 m for open roof ponds (as the one in this study) and 0.05 for roof ponds with gunny bags. Sharifi et al. [23] noted a range from 0.05 to 0.75 m depending on whether the system is open or covered. Pearlmutter and Berliner [29] used a water depth of 0.05 for a concrete roof and a shaded pond in a dry climate. They achieved a 15 °C drop-down of maximum temperatures for a covered pond and 10 °C for the uncovered pond.

In this study, a 0.05 m water depth was used for the roof pond and the floating fiber (gunny bags) over a concrete roof permanently uncovered day and night. The differences in mean values were less than 3% between the roof pond, floating fiber, and wet fabric. This finding indicates that it is possible to minimize the water layer of the pond and maintaining similar cooling results.

In terms of thermal performance, the wet fabric presented the highest maximum reduction versus the reference cell (0.5 °C–2.5 °C depending on the climatic condition). This outcome is not greater than Pearlmutter and Berliner [29]. The differences were noted in two factors: the permanent exposure of the wet fabric to the solar irradiance and the humid climate that reduces the evaporation rate, thus presenting less cooling performance.

In similar climatic conditions as mentioned by Spanaki et al. [46], the wet fabric presented an almost equal range of reduction of maximum values. Spanaki et al. found a maximum reduction of 2.7 °C, but the difference was that their system included a covered pond.

5. Conclusions

The use of roof ponds as evaporative cooling systems is widely investigated world-wide, especially in arid and temperate climates. However, only some variants of the system have been studied for hot and humid conditions. This follows the idea that high humidity in the air reduces the capacity of the system to evaporate water, hence, reducing the ability to cool.

Most of the systems used in humid climates include covered ponds or shaded ponds that reduce to zero the solar heat gain and leave the system to cool down by all the possible means. This kind of arrangement precludes walking or using the area above the roof as well as requires an additional structure prepared to receive extra loads of the system.

This paper presented a comparison between a classic open or unshaded roof pond, a floating fabric also known as gunny bags, and a novel variation of an evaporative cooling system of wet fabric. The objective was to identify the thermal performance of the wet fabric to achieve, at least, the same performance as the other two systems. In the end, the wet fabric showed better performance than the other systems for all the sub-humid climatic conditions and similar performance in humid conditions. The main results from this study are summarized as:

- (1) The water layer was reduced from 5 to 0.3 cm with a performance equal to or better than the other two water devices. Under low humidity conditions, the fiber increased the evaporation rate, presenting lower temperatures than the roof pond and the floating fabric. However, in the high RH season, the temperatures were similar in all three devices.
- (2) The thermal swing of all cases was similar regardless of the effect of the water layer. In all climatic conditions, the three devices maintained a thermal swing between 1.9 °C and 3.4 °C, whereas the reference cell presented a thermal swing of 4.4 °C in the seasons of lower RH. This indicates that the thermal swing of the indoor air is influenced by the concrete layer, where the most significant influence of thermal inertia occurs.
- (3) The wet fabric achieves the lowest maximum and average temperatures inside the cells in the three climatic conditions. In dry conditions, the wet fabric presented maximum temperatures of up to 2.5 °C below the reference cell and 6.6 °C below

the outside. In humid conditions, it showed 0.4 °C and 5.1 °C reductions below the reference cell and outdoor, respectively.

- (4) In terms of TDR, the wet fabric presents better performance than the other systems, achieving between 41% and 45% reduction in the three seasons, above the values of the roof pond and the floating fiber.

In addition to presenting the best performance, it provides other attractive features. First, it reduces the structural loads to be considered for adding water over the roofs. Second, it offers a walkable option in the roofs, thanks to the removal of the water layer. Third, it eliminates the vent valve to avoid flooding on the roof as it takes advantage of the current rainfall slope. Fourth, it can be applied on roofs with a slope, in comparison with the roof pond that requires a flat roof. Finally, it reduces the maintenance costs of other systems by reducing the amount of static water inside the pond.

In the future, cost-benefit studies should be directed as reduction water-use studies in order to upgrade the system and identify improvements for humid climates where the use of water is not an issue. Enhancing components of the system should be an important matter of study as the water used (greywater for instance), the porous media (fabric), and the amount of water (waste).

Author Contributions: Conceptualization, C.J.E.-L.; methodology, C.J.E.-L.; software, C.E.-d.P.; formal analysis, C.J.E.-L. and C.E.-d.P.; investigation, C.J.E.-L., K.M.A.-O. and M.E.G.-T.; writing—original draft preparation, C.J.E.-L. and C.E.-d.P.; writing—review and editing, K.M.A.-O. and M.E.G.-T.; visualization, C.E.-d.P., K.M.A.-O. and M.E.G.-T.; supervision, C.E.-d.P.; project administration, C.J.E.-L. All authors have read and agreed to the published version of the manuscript.

Funding: This research received no external funding.

Conflicts of Interest: The authors declare no conflict of interest.

Abbreviations

IECS	Indirect Evaporative Cooling System	
DBT	Dry Bulb Temperature	°C
RH	Relative Humidity	%
PRP	Psychrometric Roof Pond	
RC	Reference Cell	
FF	Floating Fiber also known as gunny bags	
WF	Wet Fabric	
RP	Roof Pond	
CPVC	Chlorinated Polyvinyl Chloride	
TDR	Temperature Difference Ratio	%
RD	Representative Day	
T	Temperature	°C
S	Thermal Swing	°C

Subscripts

maxout	outside maximum
maxin	inside maximum
minout	outside minimum
mdaily	mean daily
mseason	mean season

References

1. Erdemir, D.; Ayata, T. Prediction of temperature decreasing on a green roof by using artificial neural network. *Appl. Therm. Eng.* **2017**, *112*, 1317–1325. [\[CrossRef\]](#)
2. La Roche, P.; Berardi, U. Comfort and energy savings with active green roofs. *Energy Build.* **2014**, *82*, 492–504. [\[CrossRef\]](#)
3. Berardi, U.; La Roche, P.; Almodovar, J.M. Water-to-air-heat exchanger and indirect evaporative cooling in buildings with green roofs. *Energy Build.* **2017**, *151*, 406–417. [\[CrossRef\]](#)

4. Al-Zubaydi, A.Y.T.; Hong, G. Experimental study of a novel water-spraying configuration in indirect evaporative cooling. *Appl. Therm. Eng.* **2019**, *151*, 283–293. [\[CrossRef\]](#)
5. Chen, Q.; Yang, K.; Wang, M.; Pan, N.; Guo, Z.-Y. A new approach to analysis and optimization of evaporative cooling system I: Theory. *Energy* **2010**, *35*, 2448–2454. [\[CrossRef\]](#)
6. Sotelo-Salas, C.; del Pozo, C.E.; Esparza-López, C.J. Thermal assessment of spray evaporative cooling in opaque double skin facade for cooling load reduction in hot arid climate. *J. Build. Eng.* **2021**, *38*, 102156. [\[CrossRef\]](#)
7. Ketan Nayak, A.; Hagishima, A.; Tanimoto, J. A simplified numerical model for evaporative cooling by water spray over roof surfaces. *Appl. Therm. Eng.* **2020**, *165*, 114514. [\[CrossRef\]](#)
8. Belarbi, R.; Ghiaus, C.; Allard, F. Modeling of water spray evaporation: Application to passive cooling of buildings. *Sol. Energy* **2006**, *80*, 1540–1552. [\[CrossRef\]](#)
9. Stanković, S.B.; Popović, D.; Poparić, G.B. Thermal properties of textile fabrics made of natural and regenerated cellulose fibers. *Polym. Test.* **2008**, *27*, 41–48. [\[CrossRef\]](#)
10. Zhang, L.; Zhang, R.; Zhang, Y.; Hong, T.; Meng, Q.; Feng, Y. The impact of evaporation from porous tile on roof thermal performance: A case study of Guangzhou's climatic conditions. *Energy Build.* **2017**, *136*, 161–172. [\[CrossRef\]](#)
11. Wang, J.; Santamouris, M.; Meng, Q.; He, B.J.; Zhang, L.; Zhang, Y. Predicting the solar evaporative cooling performance of pervious materials based on hygrothermal properties. *Sol. Energy* **2019**, *191*, 311–322. [\[CrossRef\]](#)
12. Kaboré, M.; Bozonnet, E.; Salagnac, P. Building and urban cooling performance indexes of wetted and green roofs—a case study under current and future climates. *Energies* **2020**, *13*, 6192. [\[CrossRef\]](#)
13. Sodha, M.S.; Singh, S.P.; Kumar, A. Thermal performance of a cool-pool system for passive cooling of a non-conditioned building. *Build. Environ.* **1985**, *20*, 233–240. [\[CrossRef\]](#)
14. Coutts, A.M.; Daly, E.; Beringer, J.; Tapper, N.J. Assessing practical measures to reduce urban heat: Green and cool roofs. *Build. Environ.* **2013**, *70*, 266–276. [\[CrossRef\]](#)
15. Shakya, P.; Ng, G.; Zhou, X.; Wong, Y.W.; Dubey, S.; Qian, S. Thermal comfort and energy analysis of a hybrid cooling system by coupling natural ventilation with radiant and indirect evaporative cooling. *Energies* **2021**, *14*, 7825. [\[CrossRef\]](#)
16. García-Solórzano, L.A.; Esparza-López, C.J.; Al-Obaidi, K.M. Environmental design solutions for existing concrete flat roofs in low-cost housing to improve passive cooling in western Mexico. *J. Clean. Prod.* **2020**, *277*, 123992. [\[CrossRef\]](#)
17. Ascione, F.; De Masi, R.F.; Santamouris, M.; Ruggiero, S.; Vanoli, G.P. Experimental and numerical evaluations on the energy penalty of reflective roofs during the heating season for Mediterranean climate. *Energy* **2018**, *144*, 178–199. [\[CrossRef\]](#)
18. Ferreira, M.; Corvacho, H. The effect of the use of radiant barriers in building roofs on summer comfort conditions—A case study. *Energy Build.* **2018**, *176*, 163–178. [\[CrossRef\]](#)
19. Chungloo, S.; Limmeechokchai, B. Application of passive cooling systems in the hot and humid climate: The case study of solar chimney and wetted roof in Thailand. *Build. Environ.* **2007**, *42*, 3341–3351. [\[CrossRef\]](#)
20. Bhamare, D.K.; Rathod, M.K.; Banerjee, J. Passive cooling techniques for building and their applicability in different climatic zones—The state of art. *Energy Build.* **2019**, *198*, 467–490. [\[CrossRef\]](#)
21. De Gracia, A.; Navarro, L.; Castell, A.; Cabeza, L.F. Energy performance of a ventilated double skin facade with PCM under different climates. *Energy Build.* **2015**, *91*, 37–42. [\[CrossRef\]](#)
22. Spanaki, A.; Tsoutsos, T.; Kolokotsa, D. On the selection and design of the proper roof pond variant for passive cooling purposes. *Renew. Sustain. Energy Rev.* **2011**, *15*, 3523–3533. [\[CrossRef\]](#)
23. Sharifi, A.; Yamagata, Y. Roof ponds as passive heating and cooling systems: A systematic review. *Appl. Energy* **2015**, *160*, 336–357. [\[CrossRef\]](#)
24. González Cruz, E.; Krüger, E. Evaluating the potential of an indirect evaporative passive cooling system for Brazilian dwellings. *Build. Environ.* **2015**, *87*, 265–273. [\[CrossRef\]](#)
25. Spanaki, A.; Kolokotsa, D.; Tsoutsos, T.; Zacharopoulos, I. Theoretical and experimental analysis of a novel low emissivity water pond in summer. *Sol. Energy* **2012**, *86*, 3331–3344. [\[CrossRef\]](#)
26. Abuseif, M.; Gou, Z. A review of roofing methods: Construction features, heat reduction, payback period and climatic responsiveness. *Energies* **2018**, *11*, 3196. [\[CrossRef\]](#)
27. Marnich, R.; LaRoche, P.; Yamnitz, R.; Carbonnier, E. Passive cooling with self-shading modular roof ponds as heat sink. *Am. Sol. Energy Soc.* **2010**, *7*, 5548–5553.
28. Krüger, E.; Fernandes, L.; Lange, S. Thermal performance of different configurations of a roof pond-based system for subtropical conditions. *Build. Environ.* **2016**, *107*, 90–98. [\[CrossRef\]](#)
29. Pearlmutter, D.; Berliner, P. Experiments with a 'psychrometric' roof pond system for passive cooling in hot-arid regions. *Energy Build.* **2017**, *144*, 295–302. [\[CrossRef\]](#)
30. Tang, R.; Etzion, Y. Cooling performance of roof ponds with gunny bags floating on water surface as compared with a movable insulation. *Renew. Energy* **2005**, *30*, 1373–1385. [\[CrossRef\]](#)
31. Da Veiga, A.P.; Güths, S.; da Silva, A.K. Evaporative cooling in building roofs: Local parametric and global analyses (Part-2). *Sol. Energy* **2020**, *207*, 1009–1020. [\[CrossRef\]](#)
32. Raeissi, S.; Taheri, M. Cooling load reduction of buildings using passive roof options. *Renew. Energy* **1996**, *1481*, 301–313. [\[CrossRef\]](#)

33. Da Veiga, A.P.; Güths, S.; da Silva, A.K. Evaporative cooling in building roofs: Theoretical modeling and experimental validation (Part-1). *Sol. Energy* **2020**, *207*, 1122–1131. [[CrossRef](#)]
34. Rincón, J.; Almaro, N.; González, E. Experimental and numerical evaluation of a solar passive cooling system under hot and humid climatic conditions. *Sol. Energy* **2001**, *71*, 71–80. [[CrossRef](#)]
35. Esparza, L.; Carlos, J.; Escobar del Pozo, C.; Gomez, A.; Gomez, A.; Gonzalez, C. Potential of a wet fabric device as a roof evaporative cooling solution: Mathematical and experimental analysis. *J. Build. Eng.* **2018**, *19*, 366–375. [[CrossRef](#)]
36. García, E. *Modificaciones al Sistema de Clasificación Climática de Köppen*, 5th ed.; México, D.F., Ed.; UNAM: Ciudad de México, México, 2004.
37. ASTM International C 1046. *Standard Practice for In-Situ Measurement of Heat Flux and Temperature on Building Envelope Components*; ASTM International: West Conshohocken, PA, USA, 2001.
38. Tang, R.; Etzion, Y. On thermal performance of an improved roof pond for cooling buildings. *Build. Environ.* **2004**, *39*, 201–209. [[CrossRef](#)]
39. Yannas, S.; Erell, E.; Molina, J.L. *Roof Cooling Techniques. A Design Handbook*; Earthscan: London, UK, 2006.
40. Doğramacı, P.A.; Aydın, D. Comparative experimental investigation of novel organic materials for direct evaporative cooling applications in hot-dry climate. *J. Build. Eng.* **2020**, *30*, 101240. [[CrossRef](#)]
41. ASTM International C 168. *Standard Terminology Relating to Thermal Insulation*; ASTM International: West Conshohocken, PA, USA, 2003.
42. ASTM International C 1155. *Standard Practice for Determining Thermal Resistance of Building Envelope Components from the In-Situ Data*; ASTM International: West Conshohocken, PA, USA, 2001; Volume 4.
43. ISO 7726; Ergonomics of the Thermal Environment-Instruments for Measuring Physical Quantities. International Organization for Standardization: Geneva, Switzerland, 1998; Volume 1998.
44. Yeom, D.; La Roche, P. Investigation on the cooling performance of a green roof with a radiant cooling system. *Energy Build.* **2017**, *149*, 26–37. [[CrossRef](#)]
45. Esparza-López, C.J.; Gómez-Amador, A.; Gómez-Azpeitia, G.; González-Cruz, E.M.; Escobar del Pozo, C. Desempeño térmico de tres dispositivos de enfriamiento evaporativo indirecto pasivo en clima cálido sub-húmedo. *Palapa* **2015**, *3*, 84–96.
46. Spanaki, A.; Kolokotsa, D.; Tsoutsos, T.; Zacharopoulos, I. Assessing the passive cooling effect of the ventilated pond protected with a reflecting layer. *Appl. Energy* **2014**, *123*, 273–280. [[CrossRef](#)]